ROADWAY SAFETY INSTITUTE

Human-centered solutions to advanced roadway safety

Vehicle Automation and Transportability of Crash Modification Factors

Gary Davis
Jingru Gao

Department of Civil, Environmental, and Geo- Engineering
University of Minnesota

Final Report

CTS 19-21

University of Minnesota
Driven to Discover℠

The University of Akron

Illinois
University of Illinois at Urbana-Champaign

Southern Illinois University Edwardsville

Western Michigan University

Technical Report Documentation Page

1. Report No.	2.	3. Recipients Accession No.
CTS 19-21		

4. Title and Subtitle	5. Report Date
Vehicle Automation and Transportability of Crash Modification Factors	July 2019
	6.

7. Author(s)	8. Performing Organization Report No.
Gary Davis, Jingru Gao	

9. Performing Organization Name and Address	10. Project/Task/Work Unit No.
Department of Civil, Environmental, and Geo- Engineering University of Minnesota 500 Pillsbury Drive SE Minneapolis, MN	CTS #2018053
	11. Contract (C) or Grant (G) No. DTRT13-G-UTC35

12. Sponsoring Organization Name and Address	13. Type of Report and Period Covered
Roadway Safety Institute Center for Transportation Studies University of Minnesota University Office Plaza, Suite 440 2221 University Ave SE Minneapolis, MN 55414	Final Report, 2018-2019
	14. Sponsoring Agency Code

15. Supplementary Notes

http://www.roadwaysafety.umn.edu/publications/

16. Abstract (Limit: 250 words)

Although the *Highway Safety Manual* (HSM) now provides empirical tools for predicting the safety consequences of highway engineering decisions, these tools represent the prevailing driver and vehicle conditions in the United States during the last few decades. As automated vehicles improve in capability and increase in market share, these conditions will change, possibly affecting the accuracy of HSM predictions. This report investigates the feasibility of using "transportability" analyses, developed by Judea Pearl and Elias Bareinboim, to assess the "transferability" of crash modification factors (CMF) to new situations. An overview in Chapter 2 concludes that transportability analysis is, in principle, possible provided one can describe a causal mechanism that explains how a CMF works. Chapter 3 then describes developing such an explanation for pedestrian hybrid beacons (PHB). In Chapter 4 the explanatory model developed in Chapter 3 is used to assess the transportability of existing estimates of PHB CMFs to a hypothetical situation where vehicles with autonomous braking are present.

17. Document Analysis/Descriptors	18. Availability Statement
Crash modification factors, Autonomous vehicles, Automatic braking, Traffic signs, Analysis	No restrictions. Document available from: National Technical Information Services, Alexandria, Virginia 22312

19. Security Class (this report)	20. Security Class (this page)	21. No. of Pages	22. Price
Unclassified	Unclassified	48	

Vehicle Automation and Transportability of Crash Modification Factors

FINAL REPORT

Prepared by:

Gary Davis
Jingru Gao
Department of Civil, Environmental, and Geo-Engineering
University of Minnesota

June 2019

Published by:

Roadway Safety Institute
Center for Transportation Studies
University of Minnesota
University Office Plaza, Suite 440
2221 University Ave SE
Minneapolis, MN 55414

ACKNOWLEDGMENTS

The funding for this project was provided by the United States Department of Transportation's Office of the Assistant Secretary for Research and Technology for the Roadway Safety Institute, the University Transportation Center for USDOT Region 5 under the Moving Ahead for Progress in the 21st Century Act (MAP-21) federal transportation bill passed in 2012. This project extends work initially done as part of a Minnesota Department of Transportation project.

TABLE OF CONTENTS

LIST OF FIGURES

LIST OF TABLES

CHAPTER 1: INTRODUCTION

Crash modification factors (CMF) are commonly defined as ratios of expected road crash frequencies caused by different treatment conditions. CMFs are key inputs to the *Highway Safety Manual's* (HSM) (AASHTO, 2010) prediction methodology, and at present the best estimates of CMFs come from before/after studies that control for regression-to-mean (RTM) bias. When several estimates of a treatment's CMF are available, perfect agreement is rare. For example, a study of the safety effect of pedestrian hybrid beacons (PHB) in Tucson, Arizona, produced an estimated CMF=0.31 (Fitzpatrick and Park, 2010), while a recent National Cooperative Highway Research Program (NCHRP) study, using data from several U.S. cities, produced an estimated CMF=0.244 (Zegeer et al., 2017). The range of the estimates also vary depending on methodological assumptions. This has led to interest as to whether, and how, a CMF estimated for one location can be applied, or transferred, to different locations with possibly different traffic and crash-generating conditions. Transferability of CMFs, which was highlighted at the recent Federal Highway Administration (FHWA) CMF Needs Assessment Workshop, is the focus of NCHRP project 17-63 (FHWA, 2015).

Hauer et al. (2012) has brought some clarity to the transferability issue. It suggested extending the statistical models that currently support CMF estimation, which treat the CMF as a constant, to allow CMFs to vary across different locations, as functions of local influences. That study provided guidance on how to combine two or more CMF estimates and how to estimate the between-location variability in CMFs. Significant between-location variability means that the transfer of an estimate from one location to another will be questionable, and the authors recommend that future studies should record and report the "relevant circumstances" that are likely to affect CMFs. How these relevant circumstances are to be identified, however, was left open. Persaud, Lyon, and Srinivasan (2015) also addressed the transferability issue, noting that "…understanding the underlying causes of variability in CMF estimates is key to success in widespread application of CMF knowledge…" That study discussed using meta-regression and cross-sectional analyses to develop CMfunctions, which express crash modification effects as functions of site or regional conditions. The authors noted, however, that "considerable challenges" remain. In fact, empirical development of CMfunctions has been a topic of research for at least a decade. Elvik (2013) described two early efforts, one looking at the effects of bypass roads and one at converting standard intersections to roundabouts. That study noted that the heterogeneity among published studies can make meta-analysis difficult, and that the lack of well-established road-safety theory hindered identification of relevant circumstances. More recently, Park et al. (2015), looking at individual sites within a geographic region, found that the safety effects of bicycle lane installations varied with certain road and traffic conditions, while Chen and Persaud (2014) reported that, when attempting to identify CMfunctions for individual sites within a geographic area, hierarchical models appeared more promising than single-level specifications.

To date, research has tended to focus on geographic transferability, that is, the possibility of applying a CMF estimated in one region to different regions, although the spatial scale has varied, from differences among individual road sites to differences among nations (e.g., Elvik, 2013). A related issue concerns

the application of a CMF estimated during current conditions to possibly different conditions in the future. This possibility of temporal transferability is becoming more important as we recognize that the empirical results supporting the HSM are largely statistical summaries of recent driver and vehicle characteristics, and that these could change significantly if and when automated vehicles (AV) improve their capabilities and increase their market share. One possibility, of course, is that the AV environment will be similar enough to existing conditions that little adjustment will be needed. At least one preliminary exploration indicates, however, that this might not be the case (Granados et al., 2018). On the other hand, the AV environment could be so different that the research supporting the HSM, spanning decades and costing millions of dollars, will become obsolete, and rational road safety engineering will start over from scratch. At least in the shorter run, something intermediate is more likely, especially when roads are populated by mixtures of AVs and traditional vehicles. This leads to the question of how the existing safety research investment might be leveraged with limited experience with AVs to support reasonable decision-making.

CMF transferability is essentially a special case of assessing the external validity of an empirical result, and roughly contemporary with the building concern about CMF transferability, researchers in other disciplines have given thought to identifying conditions that warrant external validity (Cartwright, 2011; Clarke et al., 2014). Especially promising is work by Pearl and Bareinboim (Pearl and Bareinboim, 2014; Barenboim and Pearl, 2013), which have described a set of formal methods for determining when a causal effect estimated in one situation might be applied, or "transported," to a different situation. These methods show how to combine prior background causal knowledge with results from controlled experiments and observational studies to predict the causal effect of a treatment in a new situation. In Chapter 2, we introduce Pearl and Bareinboim's transportability methods to the CMF transferability problem by considering two simple but plausible scenarios. These examples illustrate how to identify "relevant circumstances," and lead to expressions for calibrating an existing CMF to reflect new conditions. In Chapter 3, we develop and test a causal model of how pedestrian hybrid beacons achieve their reported crash modification effects. In Chapter 4, we then apply the results from Chapter 2 to the model developed in Chapter 3, to assess the transportability of the PHB CMF to hypothetical situations where automated vehicles are present. A note on terminology: "transferability" and "transportability" are approximate but not perfect synonyms; because we focus here on applications of Pearl and Bareinboim's transportability methods, we will tend to use that term in preference to "transferability."

CHAPTER 2: TRANSPORTABILITY OF CAUSAL EFFECTS

2.1 GRAPHICAL MODELS

Transportability analysis is essentially a continuation of the project begun by Judea Pearl over 30 years ago, which sought to develop and extend formal reasoning tools that support uncertain causal inference. To illustrate Pearl's approach, let Y denote a random variable describing an outcome of interest, and X be a random variable which has a possible influence on Y. The observational association between X and Y is then characterized by the standard conditional probability P(Y=y|X=x). The causal effect of X on Y is the outcome observed after experimentally manipulating X, and this is denoted by P(Y=y|do(X=x)). These two probabilities might be the same but the old caution that "correlation does not imply causation" tells us not to expect this. A central problem then is to identify conditions where observational studies that estimate conditional probabilities are also sufficient to identify causal effects, and this generally requires leveraging observational results with background knowledge about causal structure. A key tool for this is the representation of background knowledge as a graph, i.e. a set of nodes and links, where the nodes represent random variables and the links indicate how the variables depend on each other. Pearl and his associates have developed a set of inference rules, called the do-calculus, by which a graphical model guides the reduction of a statement about causal effects, involving do(.) operations, to an equivalent expression involving conditional and unconditional probabilities, which could in principle be estimated from observational studies.

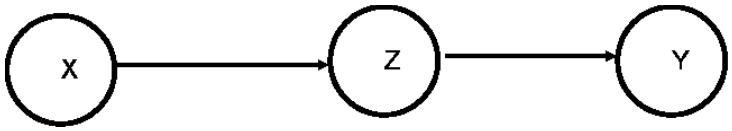

Figure 2. 1 Graphical model for a simple three-variable system.

To illustrate, let X, Y, and Z denote three random variables related according to the graphical model shown in Figure 2. 1. Here, Y is dependent on Z, while Z is dependent on X. For example, Y could denote an outcome of interest, such as crash frequency, while X denotes a safety-related treatment. In Figure 2. 1 Z denotes a mediator, such as traffic speeds. The model in Figure 2.1 states that X directly affects Z and X indirectly affects Y through Z. All joint probability distributions consistent with Figure 2. 1 can be factored into P(X,Z,Y) = P(Y|Z)P(Z|X)P(X), and one of the cornerstones of Pearl's methodology is a relationship between the connectivity properties of a graph and the conditional dependencies among the represented random variables. In Figure 2. 1, note that node Z blocks all paths from X to Y, and so Z is said to d-separate X and Y. Since d-separation in the graph is equivalent to conditional independence in a corresponding joint probability distribution (Pearl 2009), this property of the graph allows us to conclude that random variables X and Y are conditionally independent given Z, which we will express as $X \perp\!\!\!\perp Y|Z$. That is, the joint conditional distribution of X and Y factors to P(X,Y|Z) = P(X|Z)P(Y|Z).

2.1.1 Graphical Models and Causal Inference

In the graphical model shown in Figure 2. 2, Y again denotes a target outcome, such as crash frequency, X again denotes a safety-related treatment, but now Z denotes a covariable, while M denotes an unobserved confounder. Figure 2. 2 can represent, for example, a confounded before/after study, where X=0 and X=1 denote respectively the absence and presence of a safety treatment, Z and Y denote before and after crash counts, and M is an unobserved common cause for Z and Y, such as a mean crash frequency which differs randomly across sites. A safety improvement program operates by observing a before crash count Z at a site and, based on this outcome, makes a decision about deploying X. An after-crash count Y is then observed and the goal is to estimate the crash modification factor that would be observed in a randomized trial of the treatment.

$$CMF = \frac{E[Y|do(X=1)]}{E[Y|do(X=0)]} \qquad (2.1)$$

Since

$$E[Y|do(X=x)] = \sum_y yP(Y=y|do(X=x))$$

determining the causal probabilities P(Y=y|do(X=x)) is sufficient to determine the CMF. It turns out that this example is essentially the Task 2 example described in Pearl (2009), and the causal probabilities can be expressed as

$$P\big(Y=y\big|do(X=x)\big)$$
$$= \sum_z P(Y=y|do(X=x),Z=z)P(Z=z|do(X=x))$$
$$= \sum_z P(Y=y|X=x,Z=z)P(Z=z)$$

The causal effects P(Y=y|do(X=x)) having been reduced to expressions involving only conditional probabilities these can now, in principle, be estimated from observational data.

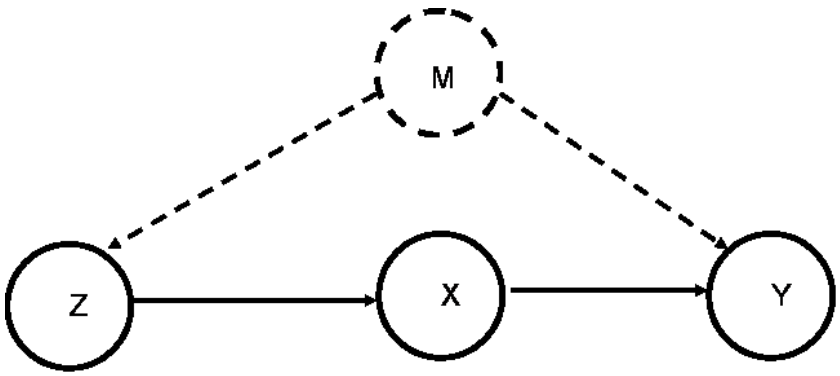

Figure 2. 2 Graphical model representing a confounded before/after study.

2.1.2 Transportability of Causal Effects

Now, suppose we are interested in a CMF for a particular site, such as a pedestrian crossing treatment. Again we'll imagine a hypothetical controlled experiment, but now a sample of n events, such as pedestrian crossing attempts, are observed without the treatment and the number of crashes recorded. The intersection is then returned to exactly the same condition as before and the treatment is installed. Another sample of n events is observed and the number of crashes is again recorded. If X=0 denotes the non-treated condition and X=1 the treated condition, while Y equals 0 or 1 depending on whether or not an event results in a crash, then Equation (2.1) becomes

$$CMF = \frac{E[Y|do(X=1)]}{E[Y|do(X=0)]} = \frac{nP[Y=1|do(X=1)]}{nP[Y=1|do(X=0)]} = \frac{P[Y=1|do(X=1)]}{P[Y=1|do(X=0)]} \quad (2.2)$$

Now, suppose a CMF has been reliably estimated for the treatment under existing vehicle and driver conditions and we wish to apply this to a new set of conditions, such as those prevailing when automated vehicles have a significant market share. To formalize such possibilities Pearl and Bareinboim introduced what they call a selection diagram, a graphical model with additional nodes and links indicating where two situations differ. Figure 2. 3 shows a selection diagram for the system represented in Figure 2. 1, where the selection node S indicates that the distribution of Z differs in the two situations. That is, if S=0 denotes our initial situation (e.g. without AVs) and S=1 denotes the new situation (e.g. with AVs) then P(Z|S=0) does not necessarily equal P(Z|S=1). If the goal is to estimate the causal effect do(X=1) in the new situation, P(Y|do(X=1), S=1), Pearl and Bareinboim's results can be used to show that this is possible, and that the transport formula is

$$P(Y=1|do(X=1),S=1) = \sum_z P(Y=1|do(X=1),S=0,Z=z)P(Z=z|do(X=1),S=1) \quad (2.3)$$

That is, the causal effect in the new situation (S=1) can be computed from the covariate-specific causal effects in the old situation P(Y=1|do(X=1), S=0,Z=z) together with the causal effect on the covariate in the new situation P(Z=z|do(X=1),S=1).

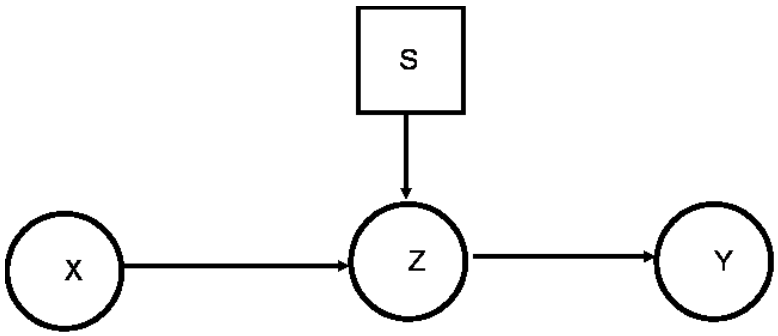

Figure 2. 3 Selection diagram indicating that the distributions for Z can differ in different situations.

2.2 TWO EXAMPLE SCENARIOS

2.2.1 Scenario 1

Figure 2. 4 shows the selection diagram for our first transportability scenario. As before Y denotes the non-occurrence (Y=0) or occurrence (Y=1) of a crash whiles X=0 and X=1 denote, respectively, the absence and presence of a safety treatment. The outcome Y depends on two inputs, U which is affected by the treatment, and V which is not. S is a selection node with S=0 and S=1 denoting the original and new situations, respectively. The selection node S pointing into V indicates that the distribution of V can differ between the two situations. For example, at a road crossing, U could stand for variables characterizing pedestrian behavior while V stands for variables characterizing vehicle and driver behavior. Figure 2. 4 then states that the intervention operates by affecting pedestrian actions, but that vehicle/driver behavior differs in the two situations being considered. Research has determined the CMF for the treatment in the current situation and we want to transport this knowledge to the new situation.

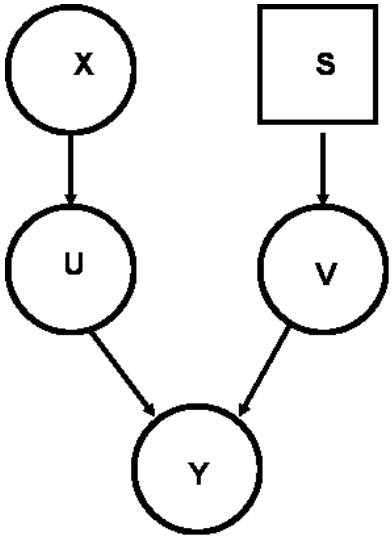

Figure 2. 4 Selection diagram for Scenario 1.

To begin, suppose that the causal effect P(Y=1|do(X=1), S=0) has been estimated in the original situation and we seek to transport this to the new situation. That is, we want P(Y=1|do(X=1),S=1). Note that, in Figure 2. 4, node V blocks the path from S to Y, so that V d-separates Y from S, which implies that that Y $\perp\!\!\!\perp$ S|V. Theorem 2 in Pearl and Bareinboim (2014) then implies that the v-specific causal effects in the original situation are directly transportable between the two situations. That is

$$P(Y = 1|do(X = 1), S = 0, V = v) = P(Y = 1|do(X = 1), S = 1, V = v)$$

Pearl and Bareinboim's (2014) Corollary 1 (Pearl and Bareinboim, 2014) then implies that a transport formula is

$$P(Y=1|do(X=1),S=1)=\sum_{v}P(Y=1|do(X=1),S=0,V=v)P(V=v|S=1) \qquad (2.4)$$

That is, in this case the v-specific causal effect estimated in the original situation, plus knowledge of how V varies in the new situation, are sufficient to transport causal knowledge from the original situation to the new situation.

The CMF for our intervention in the new situation is

$$CMF^{*}=\frac{P[Y=1|do(X=1),S=1]}{P[Y=1|do(X=0),S=1]} \qquad (2.5)$$

so applying Equation (2.4) to the numerator and denominator of Equation (2.5) can lead to an estimator of CMF*, the CMF for the new situation. This would, however, require determining not just average causal probabilities P(Y=1|do(X), S=0) in the original situation but also how these vary as V varies. For example, at a pedestrian crossing, where V denotes vehicle speed, we would need a function that relates the causal effect of the treatment on pedestrian crash risk to vehicle speed. For rare events such as road crashes even obtaining a sample size sufficient to estimate the average effect P(Y=1|do(X), S=0) can be difficult, and samples sufficient to estimate v-specific effects will often be impractical. This is a common situation when rare events are of interest, and a common solution is a retrospective study. For estimating CMFs, a variant of a retrospective analysis was suggested in Davis (2014), which can be applied here when it is possible to estimate the distribution of V in the population of crashes. To see this, note again that, in Figure 2. 4, V d-separates S from Y, and that X is a root node (i.e. has no arrows pointing into it), so Pearl's do-calculus implies

$$P[Y=1|do(X=1),V=v,S=1)=P(Y=1|X=1,V=v)=P(Y=1|do(X=1),V=v,S=0).$$

Applying Bayes Theorem gives us

$$P(Y=1|X=1,V=v,S=0)=\frac{P(V=v|Y=1,X=1,S=0)P(Y=1|X=1,S=0)}{P(V=v|X=1,S=0)} \qquad (2.6)$$

Substituting Equation (2.6) into (2.4) and (2.5), and simplifying, leads to

$$CMF^{*}=(CMF)\left(\frac{\sum_{v}\left(\frac{P(V=v|Y=1,X=1,S=0)}{P(V=v|S=0)}\right)P(V=v|S=1)}{\sum_{v}\left(\frac{P(V=v|Y=1,X=0,S=0)}{P(V=v|S=0)}\right)P(V=v|S=1)}\right) \qquad (2.7)$$

Equation (2.7) states that, for systems represented by the graph in Figure 2. 4, the transported CMF equals the original CMF multiplied by a calibration factor that depends on the distribution of V-values in the populations of crashes, and on the distributions of V in the original and new situations. If retrospective data on crashes are available this offers a potentially practical method for transporting a CMF.

2.2.1.1 Computational Example for Scenario 1

To illustrate these results, suppose that the treatment of interest affects pedestrian behavior at a road crossing and that we wish to transport a current estimate, made when automated vehicles were absent, to a situation where they are present. That is, X=0 and X=1 respectively denote to absence or presence of the treatment, while S=0 and S=1 denote situations without and with AVs. For simplicity, we will assume that U and V are also binary-valued, with

$$U = \begin{cases} 0, careful\ pedstrian \\ 1, careless\ pedestrian \end{cases} \qquad V = \begin{cases} 0, careful\ driver \\ 1, careless\ driver \end{cases}$$

and that a crash occurs if either the pedestrian is careless, or if the pedestrian is careful but the driver is careless. Formally

$$Y = \begin{cases} 0, & U = 0 \wedge V = 0 \\ 1, & U = 1 \vee (U = 0 \wedge V = 1) \end{cases}$$

Finally, let the probability distributions for U and V be given as in Table 2. 1.

Table 2. 1 Scenario 1 probability distributions for U and V as functions of X and S

		U=					V=	
		0	1				0	1
X=	0	.5	.5		S=	0	.5	.5
	1	.8	.2			1	.8	.2

The effect of the treatment is to increase the fraction of careful pedestrians, while the presence of AVs increases the fraction of careful drivers.

Computations for this example are detailed in the Appendix. Using the definition of Y and the probabilities in Table 2. 1, direct computation of the CMFs gives us:

$$CMF = \frac{P(U = 1 \vee (U = 0 \wedge V = 1) | S = 0, X = 1)}{P(U = 1 \vee (U = 0 \wedge V = 1) | S = 0, X = 0)} = \frac{.2 + (.8)(.5)}{.5 + (.5)(.5)} = 0.8$$

$$CMF^* = \frac{.2 + (.8)(.2)}{.5 + (.5)(.2)} = 0.6$$

So in this example the treatment, which increases the fraction of careful pedestrians, has a greater reduction effect when AVs are present. To apply Equation (2.7) we need the distributions of V in crashes occurring with and without the intervention. These are

$$P(V = 0 | Y = 1, X = 1, S = 0) = 0.167$$
$$P(V = 1 | Y = 1, X = 1, S = 0) = 0.833$$
$$P(V = 0 | Y = 1, X = 0, S = 0) = 0.333$$

$$P(V = 1|Y = 1, X = 0, S = 0) = 0.667$$

Substituting these into Equation (2.7), along with V distributions taken from Table 2. 1 leads to

$$CMF^* = (.8)\left(\frac{.6}{.8}\right) = 0.6$$

So here we have an example of a CMF estimated in one condition being re-calibrated to reflect new conditions. Accomplishing this required (1) formulating a graphical model for the crash-generating process, (2) identifying those variables which are expected to change between the original and the new situations, and (3) identifying a set of variables that d-separate the situational changes from the crash outcome. This then allowed us to determine what features of the original situation could be transported to the new one (the distribution of careless vs careful drivers involved in crashes) and what features of the new situation needed to be predicted (how the overall distribution of careless vs careful drivers would change between the situations).

2.2.2 Scenario 2

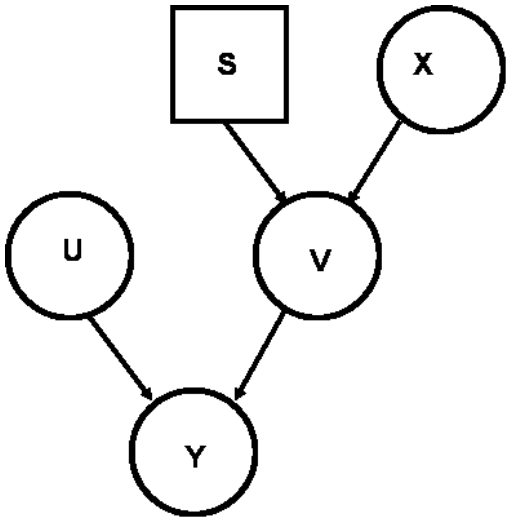

Figure 2. 5 Selection diagram for Scenario 2.

Figure 2. 5 shows the selection diagram for our second scenario, similar to the first except that now V is affected both by the treatment and by the changes between the two situations. An example might be a pedestrian crossing improvement that affects driver behavior which is also expected to change when AVs are present. As before, our goal is to estimate the CMF in the new situation

$$CMF^* = \frac{P(Y = 1|do(X = 1), S = 1]}{P(Y = 1|do(X = 0), S = 1]}$$

Starting with the numerator we can use Pearl's do-calculus to derive the transport formula

$$P[Y = 1|do(X = 1), S = 1]$$

$$= \sum_v P(Y = 1|do(X = 1), S = 1, V = v)P(V = v|do(X = 1), S = 1)$$

$$= \sum_v P(Y = 1|do(X = 1), S = 1, V = v)P(V = v|X = 1, S = 1) \quad do - calculus\ Rule\ 2$$

$$= \sum_v P(Y = 1|S = 1, V = v)P(Y = v|X = 1, S = 1) \quad do - calculus\ \ Rule\ 3$$

$$= \sum_v P(Y = 1|S = 0, V = v)P(V = v|X = 1, S = 1) \quad Y \perp S|V$$

So, as with Scenario 1, v-specific effects estimated in the original scenario, and the effect of the intervention on V in the new scenario, are needed to estimate the new causal effect.

It is also possible to derive an analog to Equation (2.7)

$$CMF^* = (CMF)\left(\frac{\sum_v \left(\frac{P(V = v|Y = 1, X = 1, S = 0)}{P(V = v|X = 1, S = 0)}\right) P(V = v|S = 1, X = 1)}{\sum_v \left(\frac{P(V = v|Y = 1, X = 0, S = 0)}{P(V = v|X = 0, S = 0)}\right) (P(V = v|S = 1, X = 0)}\right) \tag{2.8}$$

We can see that, in this case, the effects of the intervention on V in the new scenario are needed to compute the calibration factor.

To illustrate, again suppose that U and V are binary-valued and that $P(U = 0) = P(U = 1) = 0.5$. The distribution of V now depends on both X and S, and let it be given in Table 2. 2.

For example, $P(V = 0|S = 0, X = 1) = 0.8$ while $P(V = 0|S = 1, X = 1) = 0.9$.

Table 2. 2 Probability distributions for V as function of both S and X

				V	
				0	1
S	0	X	0	.5	.5
			1	.8	.2
	1	X	0	.8	.2
			1	.9	.1

It is straightforward to compute directly

$$CMF = \frac{P(Y = 1|S = 0, X = 1)}{P(Y = 1|S = 0, X = 0)} = \frac{P(U = 1 \vee (U = 0 \wedge V = 1)|S = 0, X = 1)}{P(U = 1 \vee (U = 0 \wedge V = 1)|S = 0, X = 0)} = \frac{.5 + (.5)(.2)}{.5 + (.5)(.5)} = 0.8$$

$$CMF^* = \frac{.5 + (.5)(.1)}{.5 + (.5)(.2)} = 0.917$$

And, applying Equation (2.8)

$$CMF^* = (.8)\left(\frac{.917}{.8}\right) = 0.917$$

So again we have a case where an existing CMF can be re-calibrated to reflect new conditions as long as sufficient retrospective data are available.

2.3 CHAPTER SUMMARY

In summary, what this chapter shows is that if one has at hand a probabilistic causal model that explains how a crash modification affects crashes, and if one can identify which model variables are affected by situational differences and how these differences are manifested, then transportability (aka transferability) of a crash modification effect can be assessed and, when feasible, a transport formula can be derived. A major obstacle to applying these insights is that, while statistical estimates of aggregate crash modification effects are plentiful, rigorous explanations of how these effects operate are almost completely non-existent. In the next chapter we will explore how the needed explanations might be posed and tested.

CHAPTER 3: DEVELOPING AN EXPLANATORY MODEL FOR A CMF

As noted in Chapter 2, if one has probabilistic causal model that explains how a CMF works and how two situations of interest differ then Pearls/Bareinboim transportability analysis can, in principle, be used to recalibrate a CMF estimated in one situation so that it is applicable to a different situation. Although predictive models can be developed by identifying and exploiting observable regularities, even when the causes of these regularities are poorly understood, developing an explanation for a CMF requires a framework for stating hypotheses about how the CMF works and for deriving testable predictions from these hypotheses. This chapter describes development of probabilistic causal model that provides a plausible, but not yet conclusive, explanation of how pedestrian hybrid beacons could achieve reported crash reductions. In Chapter 4, Pearl/Bareinboim transportability analysis will be applied to this model.

3.1 PEDESTRIAN HYBRID BEACONS AND CRASH MODIFICATIONS

A pedestrian hybrid beacon (PHB) is "a special type of hybrid beacon used to warn and control traffic at an unsignalized location to assist pedestrians in crossing a street or highway…" (FHWA, 2011). There is reasonable statistical evidence indicating that installation of PHBs at uncontrolled crossings can reduce the frequency of pedestrian crashes. In an empirical Bayes before/after study of PHBs installed at 21 sites in Tucson, AZ, Fitzpatrick and Park (2010) reported an estimated CMF for pedestrian crashes of 0.308 (69.2% reduction), with an associated standard error of 0.155. In another empirical Bayes before/after study using 27 PHB sites, some of which were also in Tucson, Zegeer et al. (2017) estimated a CMF of 0.244 (75.6% reduction) for pedestrian crashes, with an associated standard error 0.128.

Many jurisdictions give right-of-way to pedestrians once they have entered a marked or unmarked crosswalk, as long as drivers are given sufficient distances to stop and as long as right-of-way is not controlled by a traffic signal. Studies using staged crossing attempts, however, have found locations where substantial numbers of approaching drivers failed to yield to pedestrians (e.g. Fitzpatrick et al., 2014; Bertulis and Dulaski, 2014). Also, reviews of vehicle/pedestrian crash reports have shown that drivers' "Failure to yield right-of-way" is frequently cited as a contributing factor (e.g. Shankar, 2003; Kimley-Horn, 2017). Finally, high rates of driver yielding have been observed at PHBs, in both before/after and in cross-sectional studies, and high rates of PHB use by pedestrians have also been reported (Fitzpatrick et al., 2014; Fitzpatrick et al., 2016). This leads to a first hypothesis about how PHBs reduce pedestrian crash frequency: at uncontrolled crossings crashes tend to occur when pedestrians attempt to cross but drivers fail to slow or stop, despite having adequate stopping distances. After the PHB is installed pedestrians tend to use it, drivers tend to stop as required, and crashes are prevented. If this is the case then it should be possible to generate CMFs similar to those reported in the literature by simulating vehicle/pedestrian encounters taking place according to the hypothesis.

If the scenario proposed by the above hypothesis is typical then this should be seen when crashes are investigated in detail. In particular, there should be no evidence of pre-impact braking on the part of drivers and the collision speeds of vehicles should tend to mirror the running speeds on the roads where crashes occurred. Regarding whether or not drivers brake when encountering pedestrians, a review of

the crash reports from an in-depth investigation of fatal pedestrian crashes in Adelaide, Australia showed pre-impact skid marks in approximately 24% of the cases, indicating that, even in very serious collisions, at least some drivers braked prior to collision (McLean et al., 1994). Regarding the relationship between impact speeds and running speeds, Figure 3. 1 plots estimated impact speed versus speed limit for vehicle/pedestrian crashes investigated in NHTSA's Pedestrian Crash Data Study (PCDS) (Chidester and Isenberg, 2001). The data shown in Figure 3. 1 are for pedestrians between ages 15 and 60 and for vehicles going straight (not turning). A fitted linear relationship between speed limit and impact speed gave an estimated slope of 0.67, indicating that the estimated impact speeds tended to be lower than speed limits, and raising the possibility that some drivers might have decelerated before collision. Finally, Randles et al. (2001) were able to estimate impact speeds from video recordings of 13 vehicle/pedestrian crashes which occurred on a busy arterial in Helsinki. The speed limit on this road was 50 km/hour but in all cases the estimated impact speeds were less than the speed limit. Overall then, these findings suggest that we should be careful about equating drivers' failure to yield to pedestrians, as seen in field studies, with a failure to brake when a collision appears imminent.

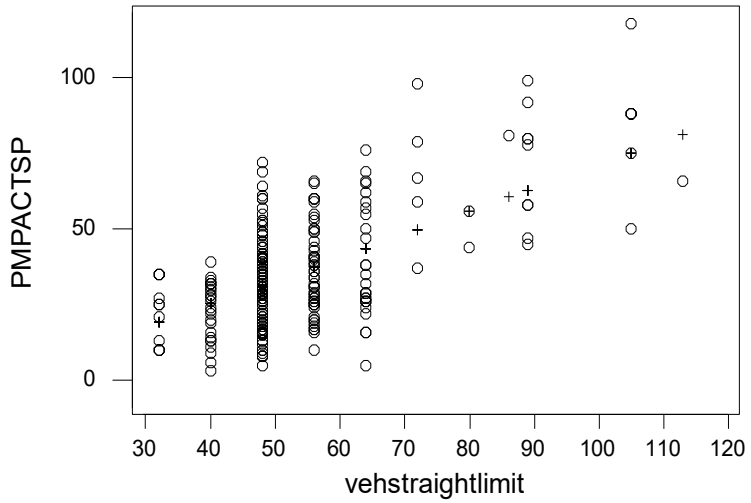

Figure 3. 1 Impact speed (y-axis) versus speed limit (x-axis) for pedestrian crashes in the PCDS.

Turning to pedestrian behavior, in the field studies staged crossings were initiated only when drivers had adequate stopping distance. The video study of pedestrian crashes in Helsinki, however, found that the crashes tended to result when pedestrians entered the roadway more or less independently of vehicle position, and that the collisions involved freely-moving vehicles, as opposed to vehicles in platoons (Pasanen and Salmivaara, 1993). This suggests that a reasonable simulation model should allow for "heedless" pedestrians as well as for evasive action on the part of drivers and should employ a traffic model that allows for a mixture of platooned and freely-moving vehicles.

3.2 SIMULATING VEHICLE/PEDESTRIAN ENCOUNTERS

Collisions between vehicles and pedestrians can occur when a pedestrian is walking or running along the edge of a road, when a pedestrian is crossing at an intersection and is hit by a vehicle turning left or right, or when a vehicle leaves the roadway and strikes a pedestrian on the roadside (Stutts et al., 1996). Crashes also occur when a pedestrian attempts to cross a road and is struck by a vehicle travelling on a straight path and, arguably, this is the type of crash a PHB should prevent. Figure 3. 2 shows a scene diagram for a crash investigated by the PCDS, where an adult pedestrian, running or jogging across a road in a crosswalk, was struck by an SUV. The relevant speed limit was 30 mph (48.4 km/hr) and the NHTSA investigators estimated the impact speed at about 19 mph (30.6 km/hr). This particular crash occurred at a signalized intersection, but it has kinematic similarities with the type of encounters a PHB is designed to address.

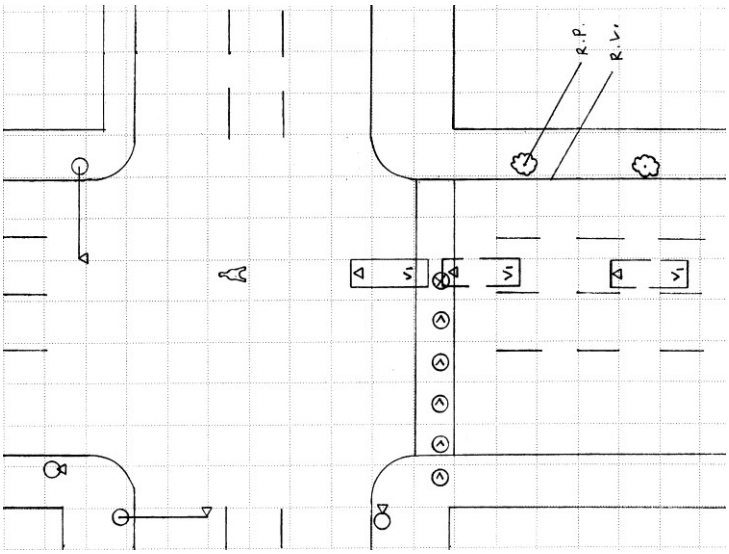

Figure 3. 2 Post-crash scene diagram from PCDS case 72639p97.

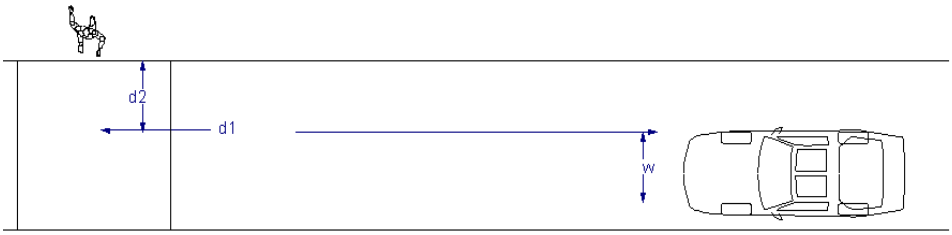

Figure 3. 3 Vehicle/pedestrian encounter at an uncontrolled crosswalk.

Microsimulation models of vehicles/pedestrian encounters have been described by Archer (2005) and by Michaud (2018). Figure 3. 3 depicts the type of event captured by our simulation model. A car, initially traveling at speed v_1, is a distance d_1 from the conflict zone when a pedestrian initiates crossing. After a reaction time r_2 the pedestrian enters the road, traveling at speed v_2. The pedestrian then enters

the conflict zone after traveling a distance d_2 from the pavement edge and exits the conflict zone after traveling a distance d_2+w from the pavement edge. If the driver takes no action then the vehicle continues at its initial speed v_1. If the driver attempts to slow or stop then, after a reaction time r_1, the vehicle begins decelerating at constant rate a_1. A crash occurs if the vehicle arrives at the conflict zone while the pedestrian is also in this zone. Otherwise, if the vehicle stops before reaching the conflict zone, or arrives either before the pedestrian enters or after the pedestrian exits the zone, a crash does not occur. If a crash occurs then v_i denotes the vehicle's speed at the point of impact. Formally:

Time pedestrian arrives in the conflict zone: $tped_1 = r_2 + \frac{d_2}{v_2}$

Time pedestrian exits conflict zone: $tped_2 = r_2 + \frac{d_2+w}{v_2}$

Vehicle's arrival time:

$$t_0 = \begin{cases} \dfrac{d_1}{v_1}, if\ no\ braking\ or\ d_1 < r_1 v_1 \\ r_1 + \dfrac{v_1 - \sqrt{v_1^2 - 2a_1(d_1 - r_1 v_1)}}{a_1}, if\ braking\ and\ r_1 v_1 \le d_1 \le r_1 v_1 + \dfrac{v_1^2}{2a_1} \\ \infty, if\ braking\ and\ d_1 > r_1 v_1 + \dfrac{v_1^2}{2a_1} \end{cases} \quad (3.1)$$

A crash occurs if $tped_1 < t_0 < tped_2$. The impact speed is then given by

$$v_i = \begin{cases} v_1, if\ no\ braking\ or\ d_1 < r_1 v_1 \\ \sqrt{v_1^2 - 2a_1(d_1 - r_1 v_1)}, if\ braking\ and\ r_1 v_1 \le d_1 \le r_1 v_1 + \dfrac{v_1^2}{2a_1} \\ 0, if\ braking\ and\ d_1 > r_1 v_1 + \dfrac{v_1^2}{2a_1} \end{cases} \quad (3.2)$$

If values for the variables d_1, v_1, r_1, a_1, d_2, v_2, r_2, w, and the driver's braking decision are known, then whether or not a collision occurs, and the resulting impact speed, can be computed using equations (3.1) and (3.2).

Equation (3.2) predicts the impact speed in a vehicle/pedestrian collision. To link the impact speed to pedestrian injury severity a logit model, developed in (Davis and Cheong, 2019) for pedestrians ages 15-60, is used. Using the KABCN injury coding system, a Possible injury corresponds to injury codes C or N, a Probable injury corresponds to codes A or B, and a Fatal injury corresponds to code K. Using injury versus impact speed data from the PCDS, supplemented by an exogenous sample of pedestrian injury severities occurring in the Twin Cities of Minnesota, the authors fit several logit models, with different assumptions about measurement error and using both frequentist and Bayesian methods. The following model, representative of those fit by Davis and Cheong, was used in the simulations:

$$P(probable \vee fatal\ injury|v_i) = \frac{\exp(0.071v_i - 1.89)}{1 + \exp(0.071v_i - 1.89)}$$
$$P(possible\ injury|v_i) = 1 - P(probable \vee fatal\ injury|v_i) \quad (3.3)$$

In Equation (3.3) v_i is the impact speed in kilometers/hour.

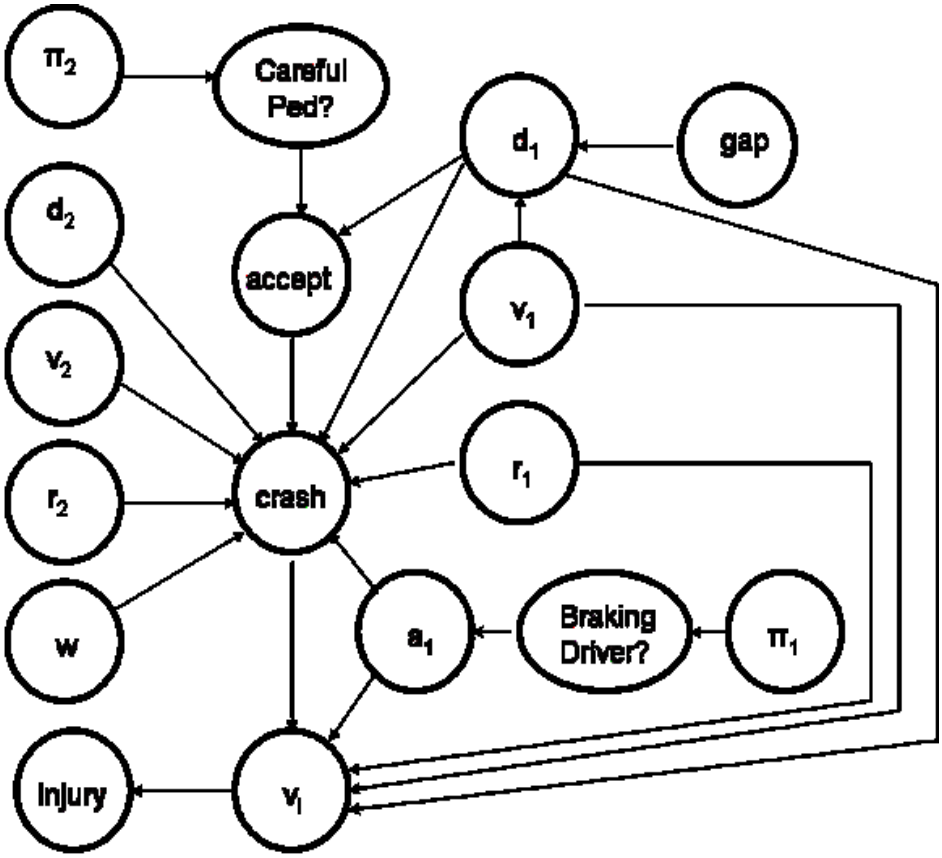

Figure 3. 4 Pedestrian crash simulation model represented as a directed acyclic graph.

Figure 3. 4 represents the simulation model as a DAG. The variable π_1 represents the fraction of braking drivers while π_2 represents the fraction of careful pedestrians. The model was coded to be run by WinBUGS (Lunn et al., 2013), a program for simulating conditional probability distributions using Markov Chain Monte Carlo. A standard Monte Carlo simulation would generate a random sample of vehicle arrivals (i.e. gaps); a subset of these would be gaps accepted by pedestrians and a subset of those would result in collisions. By using WinBUGS ability to condition on specific outcomes, such as a gap being accepted, it is possible to simulate only vehicle-pedestrian encounters, and so estimate the probability that a pedestrian is involved in a collision rather than the probability that a traffic gap results in one. The model was set up to simulate vehicle/pedestrian encounters on a hypothetical two-lane road, with both lanes being 12-feet (3.6 meters) wide. Originally, encounters in both lanes were simulated but since almost all simulated collisions occurred in the far lane interest was focused there. Traffic headways followed a shifted exponential distribution, with a minimum headway of 2 seconds and the flow of freely-moving (non-platooned) traffic was 200 vehicles/lane/hour. The nominal speed limit was 30 mph

(48.4 km/hr) and vehicle speeds were treated as normal random outcomes with a mean speed of 35 mph (56.5 km/hr) and a standard deviation of 5 mph (8.1 km/hr). Driver reaction times were treated as lognormal random outcomes with a mean of 1.07 seconds and a standard deviation of 0.248 seconds, consistent with findings reported by Koppa et al. (1997) in tests of surprised emergency braking. Driver braking decelerations were treated as lognormal outcomes with a mean of 0.63g and a standard deviation of 0.08g, again consistent with statistics from Koppa et al. (1997). Pedestrian walking speeds were taken to be normal random outcomes with a mean of 5.0 feet/second (1.52 meters/second) and a standard deviation of 0.9 feet/second (0.27 meters/second), roughly consistent with the data for "non-elderly" pedestrians reported by Fugger et al. (2001). The pedestrian reaction time r_2 was set to zero, meaning that a driver's reaction phase began at the moment the pedestrian entered the roadway.

3.3 DEVELOPING EXPLANATIONS

Table 3. 1 Simulated vehicle/pedestrian collision probability as a function of proportions of braking drivers and careful pedestrians

		Fraction of careful pedestrians (π_2)					
		0	.2	.4	.6	.8	1
Fraction of braking drivers (π_1)	0	.0629	.05632	.04969	.04305	.03622	.02867
	.2	.05093	.0461	.04076	.03531	.02953	.02315
	.4	.03987	.03594	.0317	.02706	.02258	.01731
	.6	.02906	.02537	.02248	.01896	.01542	.01157
	.8	.01766	.01521	.01322	.01089	.008484	.005853
	1	.006392	.005428	.0042	.002722	.001486	.00008627

As noted above, the initial hypothesis is that the staged pedestrian crossings used in field studies are representative of pedestrian behavior and that drivers' failure to brake when encountering pedestrians is a main cause of collisions. PHBs then reduce the frequency of collisions by increasing the fraction of braking drivers. If this hypothesis is accurate it should be possible to simulate observed CMFs by changing the fraction of braking drivers. In the simulation model a careful pedestrian was defined as being similar to the staged pedestrians in Brewer et al. (2015), accepting a gap only if the vehicle's initial distance (d_1) was greater than the AASHTO design stopping distance, 200 feet (61 meters) for a 30 mph (48.6 km/hr) speed limit. A careless pedestrian accepted the first gap greater than the following headway for platooned vehicles, 2.0 seconds. A braking driver was defined as one who, after reaction time r_1, decelerated at rate a_1, while a non-braking driver maintained a constant speed v_1.

Again letting π_1 denote the fraction of braking drivers and π_2 denote the fraction of careful pedestrians, WinBUGS was used to simulate crash occurrences for different combinations of π_1 and π_2. For each combination, 500,000 accepted gaps were simulated and the number that resulted in crashes according to Equation (3.1) recorded. These simulated crash probabilities are displayed in Table 3. 1.

Since a crash modification factor can be interpreted as the ratio of crash probabilities from two different situations (Davis, 2014) the collision probabilities listed in Table 3. 1 can be used to compute the simulated CMFs that would result from changes in driver or pedestrian behavior. For example, if before a PHB is installed, 100% of pedestrians are careful but no drivers brake, while after the PHB is installed all pedestrians are still careful but now 80% of drivers brake, the associated CMF would be

$$CMF = \frac{Collision\ Probability\ After}{Collision\ Probability\ Before} = \frac{.005853}{.02867} = 0.204 \qquad (3.4)$$

If we accept simulated CMFs between 0.2 and 0.35 as being roughly consistent with the CMFs estimated in the before/after studies then the initial hypothesis, that pedestrians are careful and that PHBs achieve their effect by increasing the fraction of braking drivers, provides an explanation of the observed CMFs. Unfortunately, though, other changes in π_1 and π_2 also lead to simulated CMFs consistent with those from the before/after studies. For example, if 80% of drivers brake both before and after installation of a PHB, but the fraction of careful pedestrians changes from 0% to 100%, the simulated CMF would be

$$CMF = \frac{Collision\ Probability\ After}{Collision\ Probability\ Before} = \frac{.005853}{.01766} = 0.331 \qquad (3.5)$$

which is again roughly consistent with the estimated CMFs. One can verify that other changes in driver or pedestrian behavior also lead to plausible CMFs. Clearly, the estimated CMFs do not by themselves provide enough information of identify a best explanation.

A good case can be made that developing an explanation is done by abductive inference, which involves a cycle of hypothesis formation, prediction, and testing of predictions (Psillos, 2002; 2011) If, in the absence of a PHB, most drivers fail to brake for pedestrians then this should be reflected in collision impact speeds, and a viable explanation should also predict impact speeds similar to those which actually occur. Lacking detailed data on impact speeds it is still possible to use pedestrian injury severity as a proxy. That is, the initial (before PHB) values for π_1 and π_2 should reproduce observed distributions of pedestrian injury severity. Toward this end, 2764 police-reported collisions between adult (ages 15-60) pedestrians and sedans, SUVs, pickups, or small vans were identified using Minnesota's Crash Mapping tool (MNCMAT). These collisions all occurred in the Twin Cities metropolitan region during the years 2008-2015. The crash records included estimates of injury severity made by the investigating officers using the KABCN system, and a summary is shown in Table 3. 2. In Table 3. 2 the 'All' column shows the injury distribution for all crashes in the sample, the "Straight-Ahead" column shows the distribution for only those crashes where the vehicles were moving forward in straight lines, and the "Straight-Ahead 30-35 mph Limit" column shows the Straight-Ahead distribution restricted to roads where the speed limit was 30 mph (48.4 km/hr) or 35 mph (56.5 km/hr).

Table 3. 2 Distribution of pedestrian injury severities: adults in MnDOT metro district

Injury Category	KABCN Range	Vehicle Movement/Speed Limit		
		All	Straight-Ahead	Straight-Ahead 30-35 mph Limit
Possible	N-C	1560 (56.4%)	573 (49.1%)	481 (51.2%)
Probable	B-A	1141 (41.3%)	551 (47.2%)	445 (47.3%)
Fatal	K	63 (2.3%)	43 (3.7%)	14 (1.5%)
Total		2764	1167	940

Let n denote the number of collisions observed (the bottom row in Table 3. 2) and Y denote the number of those collisions resulting in Possible injuries. If collisions are independent of each other Y will be a binomial random variable with probability parameter

$$P(\pi_1, \pi_2) = P(Possible|\pi_1, \pi_2) = \int P(Possible|v_i) f(v_i|\pi_1, \pi_2) d\, v_i \qquad (3.6)$$

and the log likelihood function for the observed number of possible injuries is proportional to

$$y ln\big(P(Possible|\pi_1, \pi_2)\big) + (n - y) ln\big(1 - P(Possible|\pi_1, \pi_2)\big) \qquad (3.7)$$

Using WinBUGS it is also possible to condition on the occurrence of a collision and so, via Equation (3.3), numerically evaluate the integral on the right-hand side of Equation (3.6). The hypothesis that no drivers brake and all pedestrians are careful leads to a probability of Possible injury of $p(\pi_1=0, \pi_2=1)=0.09$, i.e. only 9% of collisions result in Possible injury, which is inconsistent with the Possible injury rows of Table 3. 2. Assuming that the observed injury distributions are due to mixes of braking drivers and careful pedestrians, one can search for combinations of values for π_1 and π_2 that best fit the observed injury distribution. Using the R2WinBUGS interface (Lunn et al., 2013) the simulation model was embedded in an R function that evaluated equation (3.7) for given values of π_1 and π_2. Using the Nelder-Mead algorithm implemented in the R function optim (Teetor, 2011) approximate maximum likelihood (ML) estimates for π_1 and π_2 were computed. When using the right-most column of Table 3. 2 (n=940 and y=481) ML estimates of $\pi_1=0.98$ and $\pi_2=0.32$ were found. The log-likelihood function was then evaluated on a grid of values surrounding the ML estimates, and Table 3. 3 shows the variation in log-likelihood when the fraction of braking drivers ranges between 0.95 and 1.0 while the fraction of careful pedestrians ranges from 0 to 1 in increments of 0.1.

Table 3. 3 shows a ridge in the likelihood function corresponding to 98% of drivers braking and between 0% and 30% of pedestrians being careful. Outside this range the associated likelihoods tend to be one or more orders of magnitude lower which implies, for non-informative priors on π_1 and π_2, that the corresponding posterior probabilities would also be at least an order of magnitude lower. The best explanation then of the injury distribution, given in the rightmost column of Table 3. 2, would be that it

results when almost all drivers brake and when the fraction of careful pedestrians ranges between roughly 0% and 30%.

Table 3. 3 Variation in the log likelihood function near its maximum

		Fraction Careful Pedestrians (π_2)										
		0	.1	.2	.3	.4	.5	.6	.7	.8	.9	1.0
Fraction Braking Drivers (π_1)	.95	-662	-663	-667	-668	-673	-678	-683	-696	-731	-796	-1086
	.96	-656	-656	-660	-660	-664	-667	-670	-680	-709	-765	-1065
	.97	-653	-653	-653	-654	-656	-658	-660	-667	-682	-731	-1061
	.98	**-651**	**-651**	**-651**	**-651**	-652	-652	-653	-654	-664	-691	-974
	.99	-655	-655	-654	-654	-661	-652	-653	-652	-652	-660	-862
	1.0	-665	-665	-666	-666	-666	-664	-669	-670	-667	-663	-652

If almost all drivers brake in response to immanent collisions both before and after installation of a PHB then the crash modification effect would be due to changes in pedestrian behavior. Fixing the fraction of braking drivers at 0.98, Table 3. 4 shows how simulated collision probabilities change as the fraction of careful pedestrians ranges from 0 to 1.0, while Table 3. 5 shows simulated CMFs associated with different changes in the fraction of careful pedestrians. Again using simulated CMFs in the interval (0.2, 0.35) as being roughly consistent with the estimates from the before/after studies, it appears that the hypothesis where 98% of drivers attempt to avoid collision by braking and the fraction of careful pedestrians changes from between 0% and 30% to between 80% and 90% can explain both the observed injury distribution and the observed CMFs.

Table 3. 4 Variation in collision probabilities and injury severities with respect to change in pedestrian behavior when 98% drivers attempt to brake

Fraction Careful Pedestrians	Collision Probability	Proportion Possible Injury
0	.0077	0.52
.1	.0069	0.52
.2	.0064	0.515
.3	.0058	0.51
.4	.0051	0.50
.5	.0043	0.49
.6	.0035	0.485
.7	.0028	0.47
.8	.0021	0.43
.9	.0014	0.37
1.0	.00062	0.155

Table 3. 5 Simulated crash modification factors resulting from increases in percentage of careful pedestrians when 98% drivers attempt to brake

		Fraction Careful Pedestrians After										
		0	.1	.2	.3	.4	.5	.6	.7	.8	.9	1.0
Fraction Careful Pedestrians Before	0	1	.90	.83	.75	.66	.56	.45	.36	**.27**	.18	.08
	.1	-	1	.93	.84	.74	.62	.51	.41	**.30**	.20	.09
	.2	-	-	1	.91	.80	.67	.55	.44	**.33**	**.22**	.10
	.3	-	-	-	1	.88	.74	.60	.48	.36	**.24**	.11
	.4	-	-	-	-	1	.84	.69	.55	.41	.27	.12
	.5	-	-	-	-	-	1	.81	.65	.49	.33	.14
	.6	-	-	-	-	-	-	1	.80	.60	.40	.18
	.7	-	-	-	-		-	-	1	.75	.50	.22
	.8	-	-	-	-	-	-	-	-	1	.67	.295
	.9	-	-	-	-	-	-	-	-	-	1	.44
	1.0	-	-	-	-	-	-	-	-	-	-	1

3.4 CHAPTER SUMMARY

In summary, in this chapter we developed an explanation of how pedestrian hybrid beacons achieve their reported crash modification effects. This was done by formulating a hypothesis about how PHBs might affect crashes, deriving predictions from that hypothesis, and then comparing the predictions to empirical observations. In this case a hypothesis that PHBs reduce crashes primarily by affecting pedestrian behavior explained both an observed distribution of injury severities and reported CMFs. Although not as yet conclusive, this explanation will be used in Chapter 4 to illustrate the transportability of a CMF to an environment having automated vehicles.

CHAPTER 4: TRANSPORTABILITY OF A CRASH MODIFCATION FACTOR FOR PEDESTRIAN HYBRID BEACONS

In this chapter the general results outlined in Chapter 2 are applied to the model developed in Chapter 3 to assess the transportability of crash modification factors associated with pedestrian hybrid beacons. As in Chapter 2 the goal is to compare a transported CMF obtained via direct computation to one obtained using recalibration. In the original (S=0) situation all vehicles are assumed to be human-operated while in the new (S=1) situation vehicles equipped with an autobraking system will also be present. The question is that, given the estimate of the PHB's CMF in the original situation at a site, and the difference between the original situation (S=0) and new situation (S=1), is it possible to estimate CMF*, the PHB's CMF in the new situation.

In this example the reaction times and braking rates for human drivers are the same as described in Chapter 3, while the hypothetical autobraking systems have shorter reaction times (normally distributed with a mean of 0.5 second and a standard deviation of 0.1 second) and a harder braking rates (normally distributed with a mean of 0.8g and a standard deviation of 0.1g). For simplicity, both the human drivers and the autobraking systems are assumed to have a 100% yielding rates. Finally, it is assumed that, in the new situation, 50% of vehicles were equipped with the proposed autobraking system.

Figure 4. 1 shows the selection diagram for the simulation example. As before, Y denotes the absence (Y=0) or presence (Y=1) of a crash while X=0 and X=1 denote the absence and presence of PHB installation, respectively. The outcome Y depends on eight inputs: "accept" which indicates whether or not the pedestrian accepts the gap, the driver reaction time r_1 and driver braking rate a_1, the vehicle initial speed v_1 and initial distance d_1, the pedestrian walking speed v_2, the pedestrian reaction time r_2, the distance from pavement edge to conflict zone d_2 and the vehicle width w. Consistent with the working explanation developed in Chapter 3 in this example it is pedestrian behavior that is assumed to be affected by the PHB. S1 and S2 are the selection nodes with Si=0 and Si=1 (i=1,2) denoting the original and new situations, respectively. S1 and S2 pointing into driver braking rate and driver reaction time indicate that the distribution of a_1 and r_1 can differ between the original and new situations.

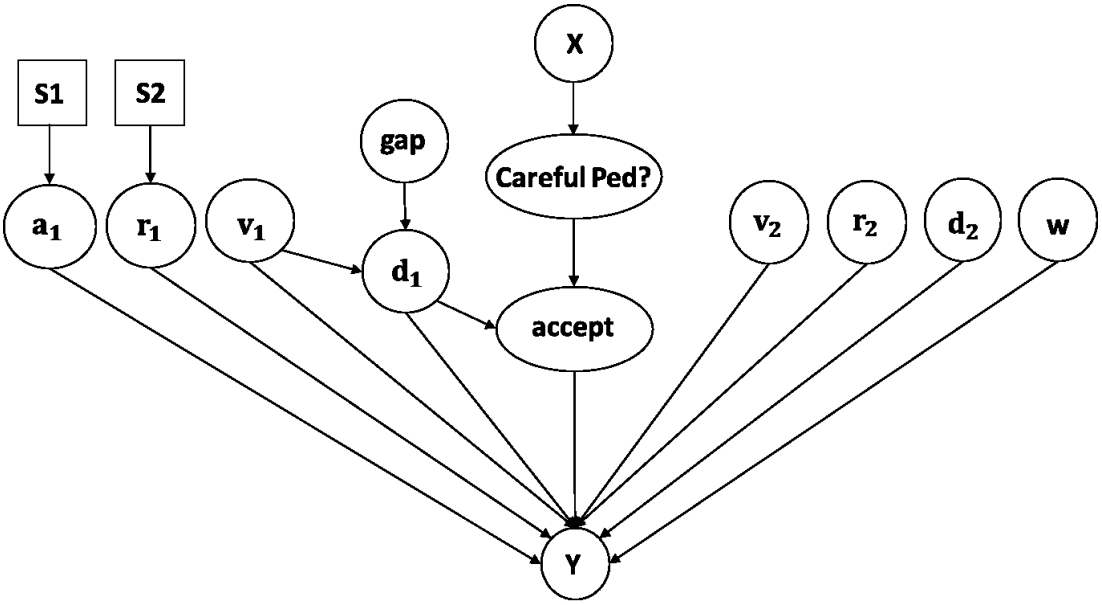

Figure 4. 1 Selection diagram for Scenario 1 case study.

As noted in Chapter 3, when almost all simulated drivers attempt to brake in vehicle-pedestrian conflicts, but the fraction of careful pedestrians changes from between 0% and 30% to between 80% and 90%, both simulated injury distributions and simulated CMFs correspond to empirical observations. In this example, the assumption is that the fraction of braking drivers is 100% and that the PHB's safety effect is to increase the fraction of careful pedestrians from 20% to 80%.

Four Markov Chain Monte Carlo (MCMC) simulations were coded and conducted using the WinBUGS program: (1) vehicle-pedestrian conflicts in the base condition (S=0) and without PHB installation (X=0); (2) vehicle-pedestrian conflicts in the base condition (S=0) but with PHB installation (X=1); (3) vehicle-pedestrian conflicts in new situation (S=1), without PHB installation (X=0); and (4) vehicle-pedestrian conflicts in new situation (S=1), with PHB installation (X=1). Key results from these four simulations are summarized in Table 4. 1.

To quantify the accuracy of the simulated crash probabilities, lower and upper bounds were computed as Posterior Mean±2×MCMC error (Lunn et al. 2013) for each posterior mean of collision probability.

The CMFs for the PHB was then computed by

$$CMF = \frac{Collision\ Probability\ After\ PHB}{Collision\ Probability\ Before\ PHB}$$

for both situations, and their accuracies were quantified using first-order approximations to the associated variances.

Table 4. 1 Key results from vehicle-pedestrian encounter simulations

		Crash probability: Without PHB	Crash probability: With PHB	CMF for PHB
Original situation (no AVs)	Mean	0.005196	0.001341	0.258083
	MCMC error	2.52E-05	1.28E-05	0.002763
	Lower bound	0.005146	0.001315	0.252556
	Upper bound	0.005246	0.001367	0.263610
New situation (50% AVs)	Mean	0.002621	0.000673	0.256810
	MCMC error	1.82E-05	9.06E-06	0.003888
	Lower bound	0.002585	0.000655	0.249034
	Upper bound	0.002657	0.000691	0.264587

In the original situation with no AVs the simulated probability of a vehicle-pedestrian collision without a PHB was 0.005196, and with a PHB this probability fell to 0.001341. In the new situation where 50% of the vehicles have autobraking, the probability of vehicle-pedestrian collision without the PHB was 0.002621, and with a PHB this probability fell to 0.0006731. The CMF associated with the PHB was 0.25808 in the no-AV situation, bounded by (0.252556, 0.263610) while that in new situation the CMF was 0.25681, bounded by (0.249034, 0.264587). That is, as might be expected, if PHBs work primarily by affecting pedestrian behavior and not driver behavior then the CMFs for PHBs should be approximately the same without and with automated vehicles.

As noted earlier, the CMF for the original situation can be transported to the new situation using Equation (2.7), which in this case takes the form:

$$CMF^{*}=CMF\frac{\sum_{a}\sum_{r_1}\frac{P((a,r_1)|Y=1,X=1,S=0)}{P((a,r_1)|S=0)}P((a,r_1)/S=1)}{\sum_{a}\sum_{r_1}\frac{P((a,r_1)|Y=1,X=0,S=0)}{P((a,r_1)|S=0)}P((a,r_1)/S=1)}$$

In words, knowledge of how a_1 and r_1 vary in crash events, with and without PHBs, can be leveraged with knowledge of how a_1 and r_1 vary in the old and new situations in order to recalibrate and existing CMF. To test this, WinBUGS was used to simulate the following conditional distributions:

(1) $P((a_1, r_1)|Y=1,X=1,S=0)$, the conditional posterior distribution of driver reaction time r_1 and driver braking rate a1, given that a crash occurred, in the original situation and without PHB;

(2) $P((a_1, r_1)|Y=1,X=0,S=0)$, the conditional posterior distribution of driver reaction time r_1 and driver braking rate a_1, given that a crash occurred, in the original situation but with PHB;

(3) $P((a_1, r_1)|S=0)$, the probability distribution of driver reaction time r_1 and driver braking rate a_1 in the original situation; and

(4) $P((a_1, r_1)|S=1)$, the probability distribution of driver reaction time r_1 and driver braking rate a_1 in the new situation.

Descriptive statistics of driver reaction time and driver braking rate from those conditional simulations are displayed in Table 4. 2.

Table 4. 2 Descriptive statistic of reaction time r_1 and deceleration rate a_1 from simulations

Quantity of Interest		Crash events in no AV situation with PHB	Crash events in no AV situation without PHB	All events original situation (No AVs)	All events new situation (50% AVs)
Driver reaction time r_1 (seconds)	Mean	1.208	1.193	1.071	0.4995
	Sd	0.288	0.2746	0.2498	0.09986
	2.5%-ile	0.7544	0.7516	0.6643	0.3033
	Median	1.171	1.165	1.043	0.4987
	97.5%-ile	1.87	1.823	1.637	0.6964
Driver braking rate a_1 (feet/second^2)	Mean	19.12	19.14	20.07	25.75
	Sd	2.32	2.367	2.547	3.238
	2.5%-ile	14.96	14.89	15.73	19.43
	Median	18.99	18.97	20.11	25.77
	97.5%-ile	24.0	24.21	25.7	32.1

Figure 4. 2 and Figure 4. 3 display the probability distributions of driver reaction time and driver braking rate in crash events in the four relevant conditions.

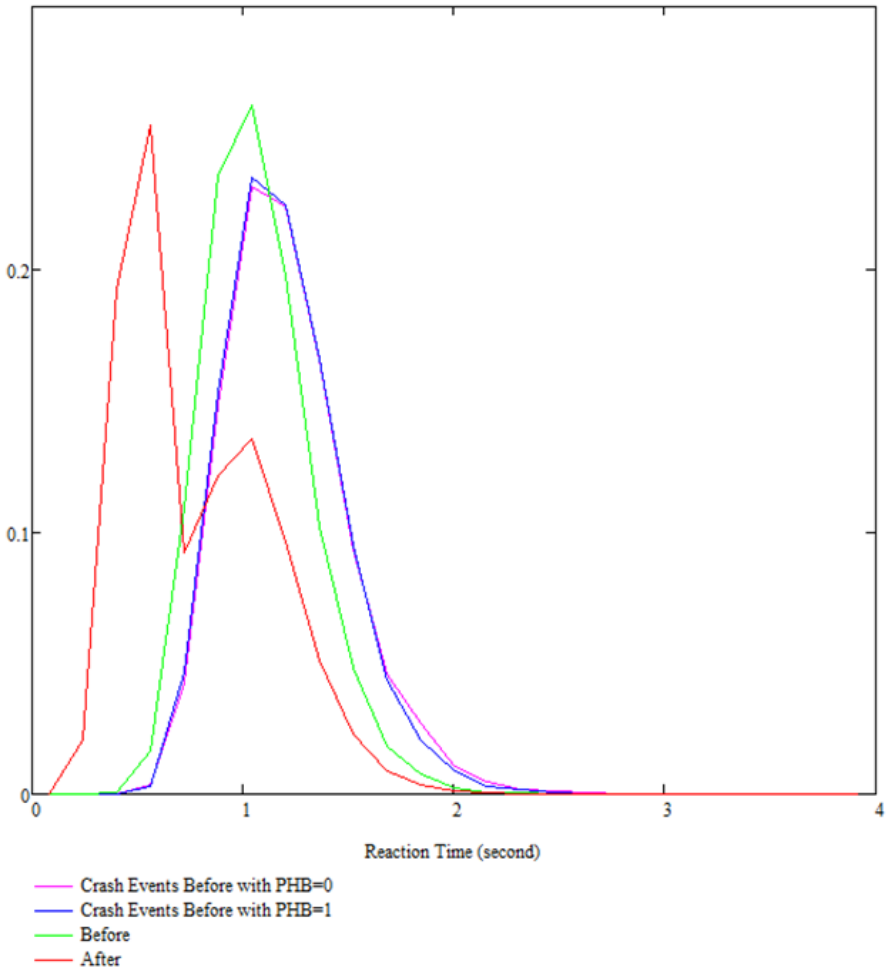

Figure 4. 2 Probability distributions of driver reaction times: for crash events without AVs both before and after PHB installation and for all events without and with AVs. Before=No AVs, After=50% AVs.

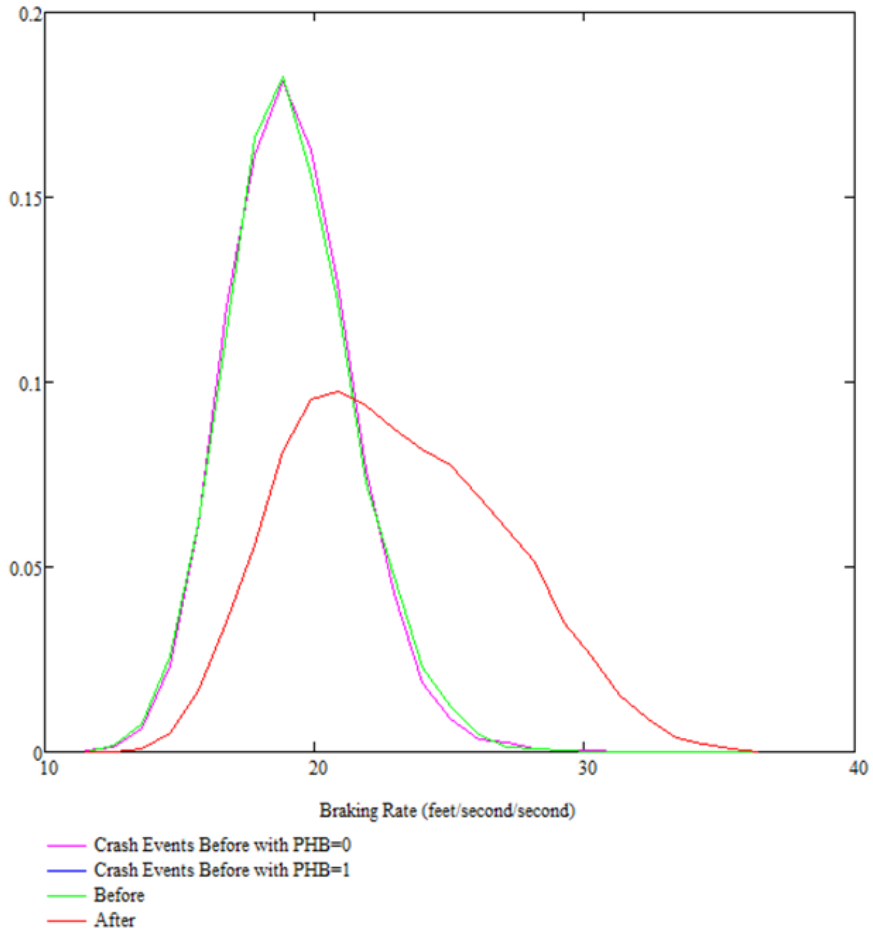

Figure 4. 3 Probability distribution of driver braking rates: for crash events without AVs both before and after PHB installation and for all events without and with AVs. Before=No AVs, After=50% AVs.

20,000 samples from each of the four MCMC simulations were used to compute the joint distributions of (a1, r_1): P((a1, r_1)|Y=1,X=1,S=0), P((a1, r_1)|Y=1,X=0,S=0), P((a1, r_1)|S=1), and P((a1, r_1)|S=0).

The CMF calibration factor, defined as

$$\frac{\sum_a \sum_{r_1} \frac{P((a,r_1)|Y=1,X=1,S=0)}{P((a,r_1)|S=0)} P((a,r_1)/S=1)}{\sum_a \sum_{r_1} \frac{P((a,r_1)|Y=1,X=0,S=0)}{P((a,r_1)|S=0)} P((a,r_1)/S=1)}$$

requires "integrating" the products of probability distributions. This was done by approximating each two-dimensional joint distribution with a two-dimensional histogram and then summing over the histograms' cells to get the numerator and denominator the calibration factor. The transported CMF* was finally computed as

$$CMF^* = CMF \times Calibration\ Factor$$

Table 4. 3 shows the CMF calibrations obtained for a range of different grids used to construct the approximating histograms.

Table 4. 3 CMF calibration factor and CMF* computation results

n	# cells	Numerator	Denominator	Calibration Factor	CMF*
10	100	0.526	0.518	1.015444	0.261985
15	225	0.52	0.512	1.015625	0.262031
20	400	0.518	0.507	1.021696	0.263598
25	625	0.513	0.503	1.019881	0.263129
30	900	0.512	0.503	1.017893	0.262616
35	1225	0.511	0.5	1.022	0.263676
40	1600	0.507	0.499	1.016032	0.262136

The transported CMF*s range from 0.261985 to 0.263676, and all fall in the interval (0.249034, 0.264587), the bounds for CMF* computed via direct simulation. This again illustrates how a transport formula such as Equation (2.7) might offer a useful method for transporting existing CMFs to new conditions.

CHAPTER 5: CONCLUSION

We began by taking note of a continuing interest in applying, or "transferring," a crash modification factor estimated for one situation to other, possibly different, situations. We also noted that this issue is likely to become more important as the mix of vehicle and driver capabilities changes with an increasing market penetration by automated vehicles. Current thinking about CMF transferability has focused on the possibility of developing CMfunctions, which describe how aggregate crash modification effects vary as aggregate measures of situational conditions vary. Here we have taken a different approach which focuses on, first, identifying sufficient conditions (aka warrants) for taking causal information determined in one situation and applying it to another situation, and second, deriving expressions for computing the transferred quantities. The analytic tools we used were Pearl and Bareinboim's "transportability" analyses, which we first applied to two simplified, but plausible, scenarios. For each of these scenarios we derived a re-calibration formula by which an existing CMF could be adjusted to reflect new conditions. We then developed a probabilistic causal model of how pedestrian hybrid beacons might achieve their reported crash modification effects, and finally used transportability analysis to assess how these CMFs might change when vehicles with a hypothetical autobraking system are present.

This report describes an exploratory analysis, leaving practical applications as topics for future work, but some comments regarding practical application are in order. The method described here has two main components. The first is a graphical model describing the dependencies among a set of relevant variables. Compared to generalized linear models, graphical models (aka Bayesian networks, or structural models) have not been used much in road safety, although applications in areas such as epidemiology, image processing, and forensic science are common (Pourret et al., 2008). One future research need then is for development and validation of graphical models for different crash scenarios. Historically, such research has been handicapped by a lack of detailed data on what actually happens during road crashes, but this situation might be improving with the availability of data from naturalistic driving studies and from in-vehicle event data recorders.

The second main component is probability distributions for model variables consistent with the graphical model. For our purposes, a full specification of the model, which includes all relevant probability distributions, might not be necessary. What is needed is the qualitative description, via a graph, in sufficient detail that we can identify a critical set of variables that d-separate the outcome from the situational differences. Actually, applying a formula such as equation (2.7) then requires distributions for these critical variables, including their distributions in populations of crash events. As noted above, data on what actually happens in crashes have historically been difficult to come by, but a promising possibility is to use information from the event data recorders typically found in airbag control modules to construct a national database that could then support transportability analyses (Chidester et al., 1999; Bonneson and Ivan, 2013).

REFERENCES

AASHTO. (2010). *Highway safety manual*. Washington, DC: American Association of State Highway and Transportation Officials.

Archer, J. (2005). *Indicators for traffic safety assessment and prediction and their application in cicro-simulation modeling: A study of urban and suburban intersections*, doctoral thesis, Royal Institute of Technology, Stockholm, Sweden.

Bareinboim, E., & Pearl, J. (2013). A general algorithm for deciding transportability of experimental results. *Journal of Causal Inference, 1*(1), 107–134.

Bertulis, T., & Dulaski, D. (2014). Driver approach speed and its impact on driver yielding to pedestrian behavior at unsignalized crosswalks. *Transportation Research Record, 2464*, 46–51.

Bonneson, J., & Ivan, J. (2013). *Theory, explanation, and prediction in road safety: Promising directions* (Transportation Research Circular, E-C179). Washington, DC: Transportation Research Board.

Brewer, M., Fitzpatrick, K., & Avelar, R. (2015). Rectangular rapid flashing beacons and pedestrian hybrid beacons pedestrian and driver behavior before and after installation. *Transportation Research Record, 2519,* 1–9.

Cartwright, N. (2011). Predicting 'It will work for us': (Way) beyond statistics. In *Causality in the sciences* Oxford, UK: Oxford University Press, 751-768.

Cartwright, N., & Hardie, J. (2012). *Evidence-based policy: A practical guide to doing it bette*r. Oxford, UK: Oxford University Press.

Chen, Y., & Persaud, B. (2014). Methodology to develop crash modification functions for road safety treatments with fully specified and hierarchical models. *Accident Analysis and Prevention, 70*, 131–139.

Chidester, A., Hinch, J., Mercer, T. C., & Schultz, K. S. (1999, May). *Recording automotive crash event data.* Presented at the International Symposium on Transportation Recorders, Arlington, VA.

Chidester, A. and Isenberg, R. (2001). Final report - the pedestrian crash data study. SAE Technical Paper 2001-06-0105.

Clarke, B., Gillies, D., Illari, P., Russo, F., & Williamson, J. (2014). Mechanisms and the evidence hierarchy. *Topoi, 33*(2), 339–360.

Davis, G. (2014). Crash reconstruction and crash modification factors. *Accident Analysis and Prevention, 62*, 294–302.

Davis, G., & Cheong, C. (2019). Pedestrian injury severity vs vehicle impact speed: Uncertainty quantification and calibration to local conditions. In *Proceedings of the Transportation Research Board 98th Annual Meeting*, Washington, DC.

Elvik, R. (2013). International transferability of accident modification functions for horizontal curves. *Accident Analysis and Prevention, 59*, 487–496.

FHWA. (2011). *Manual of uniform traffic control devices*. Washington, DC: Federal Highway Administration.

FHWA. (2015). *Summary report: Crash modification factors needs assessment workshop (No. FHWA-HRT-15-020)*. Washington, DC: Federal Highway Administration.

Fitzpatrick, K., & Park, E. (2010). *Safety effectiveness of the HAWK pedestrian crossing treatment (No. FHWA-HRT-10-042)*. Washington, DC: Federal Highway Administration.

Fitzpatrick, K., Iragavarapu, V., Brewer, M., Lord, D., Hudson, J., Avelar, R., & Robertson, J. (2014). *Characteristics of Texas pedestrian crashes and evaluation of driver yielding at pedestrian treatments (No. FHWA/TX-13/0-6702-1)*. Washington, DC: Federal Highway Administration.

Fitzpatrick, K., Avelar, R., Pratt, M., Brewer, M., Robertson, J., Lindheimer, T., & Miles, J. (2016). *Evaluation of pedestrian hybrid beacons and rapid flashing beacons (No. FHWA Report HRT-16-040)*. Washington, DC: Federal Highway Administration.

Fugger, T., Randles, B., Wobrock, J., Stein, A., & Whiting, W. (2001). *Pedestrian behavior at signal-controlled crosswalks (SAE Technical Paper No. 2001-01-0896)*. Warrendale, PA: SAE Inc.

Granados, M., Persaud, B., Rajeswaran, T., & Saleem, T. (2018). Using microsimulation to evaluate the impact of automated vehicles on safety performance of signalized intersections *(No. 18-05956)*. In Proceedings of the *Transportation Research Board 97th Annual Meeting*, Washington, DC.

Hauer, E., Bonneson, J., Council, F., Srinivasan, R., & Zegeer, C. (2012). Crash modification factors foundational issues. *Transportation Research Record, 2279,* 67–74.

Kimley-Horn. (2017). *2017 City of Minneapolis pedestrian crash study*. Retrieved from https://lims.minneapolismn.gov/Download/RCA/2877/Minneapolis-Pedestrian-Crash-Study_2017.pdf

Koppa, R. J., Fambro, D. B., & Zimmer, R. A. (1997). Measuring driver performance in braking maneuvers. *Transportation Research Record, 1550,* 8–15.

Lunn, D., Jackson, C., Best, N., Thomas, A., & Spiegelhalter, D. (2013). *The BUGS book: A practical introduction to Bayesian analysis*. Boca Raton, FL: CRC Press.

Michaud, D. (2018*) Driver distraction in microsimulation of a mid-block pedestrian crossing*, master's thesis, Portalnd State University, Portland, OR.

McLean, A., Anderson, R., Farmer, M., Lee, B, & Brooks, C. (1994). *Vehicle travel speeds and the incidence of fatal pedestrian collisions (volume II)*. Adelaide, Australia: Road Accident Research Unit, University of Adelaide.

Park, J., Abdel-Aty, M., Lee, J., & Lee, C. (2015). Developing crash modification functions to assess safety effects of adding bike lanes for urban arterials with different roadway and socio-economic characteristics. *Accident Analysis and Prevention, 74,* 179–191.

Pasanen, E., & Salmivaara, H. (1993). Driving speeds and pedestrian safety in the city of Helsinki. *Traffic Engineering and Control, 34*(6), 308–310.

Pearl, J. (2009). *Causality: Models, reasoning, and inference (2nd edition)*. Cambridge; NY: Cambridge University Press.

Pearl, J., & Bareinboim, E. (2014). External validity: From do-calculus to transportability across populations. *Statistical Science, 29*(4), 579–595.

Persaud, B., Lyon, C., & Srinivasan, R. (2015). *On the transferability of crash modification factor highway geometric design elements*. Presented at the 5th International Symposium on Highway Geometric Design, Vancouver, Canada.

Pourret, O., Naïm, P., & Marcot, B. (2008). *Bayesian networks: A practical guide to applications (Statistics in practice)*. Hoboken, NJ: John Wiley.

Psillos, S. (2002). Simply the best: A case for abduction. *Lecture Notes in Computer Science*, *2408*(2), 605–625.

Psillos, S. (2011). An explorer upon untrodden ground: Peirce on abduction. *Handbook of the History of Logic, 10*, 117–151.

Randles, B., Fugger, T., Eubanks, J., & Pasanen, R. (2001). *Investigation and analysis of real-life pedestrian collisions (SAE Technical Paper 2001-01-0171)*. Warrendale, PA: SAE Inc.

Shankar, U. (2003). *Pedestrian roadway datalities (Report DOT HS 809456)*. Washington, DC: National Highway Traffic Safety Association.

Stutts, J. C., Hunter, W. W., & Pein, W. E. (1996). Pedestrian-vehicle crash types: An update. *Transportation Research Record, 1538*, 68–74.

Teetor, P. (2011). *R cookbook (1st edition)*. Beijing: O'Reilly.

Zegeer, C., Srinivasan, R., Lan, B., Carter, D., Smith, S., Sundstrom, C., …. & Van Houten, R. (2017). *Development of crash modification factors for uncontrolled pedestrian crossing treatments (NCHRP Report 841)*. Washington, DC: National Academies.

APPENDIX A

COMPUTATIONS FOR THE SCENARIO 1 EXAMPLE

First, using the values in Table 2. 1 it is straightforward to verify that the original and new CMFs are

$$CMF = \frac{P(Y=1|S=0,X=1)}{P(Y=1|S=0,X=0)} = \frac{P(U=1 \vee (U=0 \wedge V=1)|S=0,X=1)}{P(U=1 \vee (U=0 \wedge V=1)|S=0,X=0)} = \frac{.2+(.8)(.5)}{.5+(.5)(.5)} = 0.8$$

$$CMF^* = \frac{.2+(.8)(.2)}{.5+(.5)(.2)} = 0.6$$

To apply Equation (2.4) we need the v-specific causal effects from the original (no- treatment) situation.

$$P(Y=1|X=1,V=0)$$
$$= P(U=1 \vee (U=0 \wedge V=1)|X=1,V=0)$$
$$= P(U=1|X=1,V=0)$$
$$= P(U=1|X=1) = 0.2$$

$$P(Y=1|X=1,V=1)$$
$$= P(U=1 \vee (U=0 \wedge V=1)|X=1,V=1)$$
$$= 0.2+(.8)(1) = 1.0$$

The numerator in Equation (2.4) is then

$$P(Y=1|do(X=1),S=1) = (.2)(.8)+(1.0)(.2) = 0.36$$

Similarly, the denominator is

$$P(Y=1|do(X=0),S=1) = (.5)(.8)+(1.0)(.2) = 0.6$$

and $CMF^* = \frac{0.36}{0.6} = 0.6$, as found earlier.

To apply Equation (2.7) we need the distributions of V in crashes occurring in the original situation, with and without the intervention. For example

$$P(V=0|Y=1,X=1,S=0) = \frac{P(Y=1 \wedge V=0|X=1,S=0)}{P(Y=1|X=1,S=0)}$$

$$P(Y=1 \wedge V=0|X=1,S=0)$$
$$= P(U=1 \wedge V=0|X=1,S=0)$$
$$= P(U=1|X=1)P(V=0|S=0) = (.2)(.5) = 0.1$$

$$P(Y=1|X=1,S=0)$$
$$= P(U=1|X=1)+P(U=0|X=1)P(V=1|S=0)$$
$$= .2+(.8)(.5)$$
$$= 0.6 P(V=0|Y=1,X=1,X=0) = \frac{.1}{.6} \approx 0.167$$

Ultimately, we get

$P(V = 0|Y = 1, X = 1, S = 0) = 0.167$
$P(V = 1|Y = 1, X = 1, S = 0) = 0.833$
$P(V = 0|Y = 1, X = 0, S = 0) = 0.333$
$P(V = 1|Y = 1, X = 0, S = 0) = 0.667$

Substituting these values into Equation (2.7)

$$\sum_v \frac{P(V = v|Y = 1, X = 1, S = 0)P(V = v|S = 1)}{P(V = v|, S = 0)} = \frac{(.167)(.8)}{.5} + \frac{(.883)(.2)}{.5} = 0.6$$

$$\sum_v \frac{P(V = v|Y = 1, X = 0, S = 0)P(V = v|S = 1)}{P(V = v|S = 0)} = \frac{(.333)(.8)}{.5} + \frac{(.667)(.2)}{.5} = 0.8$$

$$CMF^* = (.8)\left(\frac{.6}{.8}\right) = 0.6$$

APPENDIX B

WINBUGS CODE FOR SIMULATION MODEL

```
model

# simulation of conflicts and crashes using random acceptance

# gap acceptance IVs=log gap, ML estimates from Minitab

# Fambro et al stats of braking and reaction times

# analytic model for clearance time

#  Cowan M3 gaps, linear alpha-q relationship

# revised crash criterion

# opposing LT sight distance model


{

#conflict point opposite leftmost receiving lane

x2hit <- 1.5*Lwmin


# arrival of opposing LT

qolt.sim<- Qpolt/3600

pblock <- 1-exp(-qolt.sim*red)

block ~ dbern(pblock)


#available sight distance model from Hussain and Easa 2016

Vwo.tau <- 1/(Vwo.sig*Vwo.sig)

Yi.tau <- 1/(Yi.sig*Yi.sig)

Yp.tau <- 1/(Yp.sig*Yp.sig)

Xe.tau <- 1/(Xe.sig*Xe.sig)

XL.tau <- 1/(XL.sig*XL.sig)

XLi.tau <- 1/(XLi.sig*XLi.sig)
```

```
vwo ~ dnorm(Vwo,Vwo.tau)

yi ~ dnorm(Yi,Yi.tau)

yp ~ dnorm(Yp,Yp.tau)

xe ~ dnorm(Xe,Xe.tau)

xl ~ dnorm(XL,XL.tau)

xli ~ dnorm(XLi,XLi.tau)

SDa.num <- (((2*Dc+nlane.minor*Lwmin)/2)+yp+yi)*(1.5*Lwmaj-vwo-xli)

SDa.denom <- xli+xe-Lwmaj+xl+vwo-xo

SDa <- (SDa.num/SDa.denom)+yp-Mmin-.5*Lwmin


# Through vehicle arrival

v.sim.mu <- v.bar*(88/60)

v.sim.tau <- 1/(v.sig*v.sig*(88/60)*(88/60))

v.sim ~ dnorm(v.sim.mu,v.sim.tau)I(1,)

v.sim.mph <- v.sim*(60/88)

qp <- Qp/3600

alpha <- max(0,1-tm*qp)

lambda <- alpha*qp/(1-tm*qp)

u ~ dunif(0,1)

gap0.sim <- tm-log((1-u)/alpha)/lambda

littleu <- step((1-alpha)-u)

gap.sim <-(1- littleu)*gap0.sim + (littleu)*tm

x.sim <- gap.sim*v.sim

# tc.tau <- 1/(tc.sigma*tc.sigma)

# tc.mu <- tc.beta0+tc.beta1*log(gap.sim)
```

```
# tc.sim ~ dlnorm(tc.mu,tc.tau)

ac ~ dunif(ac.lo,ac.hi)

tc.sim  <- sqrt(2*xc/ac)

linmod.sim <- beta0 + beta1*log(gap.sim)

logit(p.sim) <- linmod.sim

# px.sim <- p.sim*step(gap.sim-gap.min)

heedless <- block*step(x.sim-SDa)

px.sim <- heedless*(1-littleu) + (1-heedless)*p.sim*step(gap.sim-gap.min)

# accept.sim <- step(p.sim-u.sim)*step(gap.sim-gap.min)

accept.sim ~ dbern(px.sim)



# collision simulation

        g <- 32.2

        # tp.sim ~dunif(0.5,1.5)

        # f.sim ~ dunif(.5,.9)


    tp.sigma2 <- log((pow(tp.sd,2)/pow(tp.bar,2))+1)

    tp.mu <- log(tp.bar)-0.5*tp.sigma2

    tp.tau <-1/tp.sigma2

    f.sigma2 <- log((pow(f.sd,2)/pow(f.bar,2))+1)

    f.mu <- log(f.bar)-0.5*f.sigma2

    f.tau <- 1/f.sigma2


    tp.sim ~dlnorm(tp.mu,tp.tau)
```

```
    f.sim ~dlnorm(f.mu,f.tau)
          a.sim <- f.sim*g
          v.sim.fps <- v.sim
      x0.sim <- x.sim+x2hit
      xbrake.sim <- pow(v.sim.fps,2)/(2*a.sim)
      xprt.sim <- v.sim.fps*tp.sim
      xstop.sim <- xbrake.sim + xprt.sim
       stop.sim <- step(x0.sim-xstop.sim)
       fullhit.sim <- step(xprt.sim-x0.sim)
       tc1.sim <- x0.sim/v.sim.fps
            vbrake2.sim <- max(v.sim.fps*v.sim.fps-2*a.sim*(x0.sim-xprt.sim),0)
       tc2.sim <-tp.sim+(v.sim.fps-sqrt(vbrake2.sim))/a.sim

       tc0.sim <- stop.sim*1000+(1-stop.sim)*fullhit.sim*tc1.sim+(1-stop.sim)*(1-fullhit.sim)*tc2.sim
# crash condition tc-crash.buffter < tc0 < tc
          close1.sim <- step(tc0.sim-(tc.sim-crash.buffer/2))*step(tc.sim+crash.buffer/2-tc0.sim)
          # hit.sim <- accept.sim*close1.sim
          phit.sim <- close1.sim*accept.sim
          hit.sim ~ dbern(phit.sim)
          v.impact <- hit.sim*((fullhit.sim*v.sim)+(1-fullhit.sim)*(sqrt(vbrake2.sim)))

}

Data    list(crash.buffer=.5,gap.min=2.5)

list(Vwo=6.7,Vwo.sig=0.1,Yi=7.7,Yi.sig=0.16,Yp=28,Yp.sig=13,Xe=1.4,Xe.sig=0.03,XL=0.2,XL.sig=1.2,XLi=2.
2,XLi.sig=0.8,Lwmaj=12,Dc=8,Lwmin=12,Mmin=10,nlane.minor=5,xo=-10,red=30)
```

list(xc=64.8,ac.lo=6.5,ac.hi=13)

list(Qp=1000,tm=2.0,Qpolt=50)

list(beta0=-8.2736,beta1=4.8475)

list(tp.bar=0.6,tp.sd=0.3,f.bar=0.75,f.sd=0.1)

list(v.bar=35.6,v.sig=9.0)

list(accept.sim=1)

list(hit.sim=1)

list(tc.beta0=.4569, tc.beta1=.31524,tc.sigma=.2799)

Inits list(u =.5,v.sim=50,block=1)